

ANISOTROPIC DEFORMATION AND ROTATION TECTONICS DURING OBLIQUE CONVERGENCE: EXAMPLES FROM NORTHEASTERN TAIWAN

CHIA-YU LU¹, TEH-QUEI LEE², JACQUES ANGELIER³, JIAN-CHENG LEE² AND HAO-TSU CHU⁴

1. Department of Geology, National Taiwan University, Taipei, Taiwan
2. Institute of Earth Sciences, Academia Sinica, Taipei, Taiwan
3. Departement de Geotectonique Univ. Pierre et Marie. Curie, Jussieu, France
4. Central Geological Survey, Taipei, Taiwan

ABSTRACT

Excellent exposures on wave-cut platforms display along the northeastern Taiwan coast a thick Oligocene succession that suffered low-grade metamorphism. The strata show anisotropic ductile-brittle deformation associated with the Late Cenozoic Taiwan mountain building event. Paleomagnetic analyses suggest probable contraction-induced remagnetization of remanent magnetization, taking place before rotation of the entire succession. Three deformation stages can be distinguished: (1) an early contraction stage that resulted in thrusting, regional tilting of strata and subsequent folding, together with remagnetization of remanent magnetization, (2) a second stage dominated by block rotation and drag folds accompanying progressive dextral shear thrusting, with domino- and bookshelf-type strike-slip fault systems as well as a variety of transpressional structures such as pressure ridges, restraining oversteps and rhomb horses and finally, (3) late transpression with little rotation represented by pop-up structures as well as penetrative pencil structure and fracture cleavage with a constant NNE-SSW orientation. This demonstrates an example of anisotropic deformation and rotation tectonics during oblique convergence at a collisional plate boundary.

Key words: anisotropic deformation, northeastern Taiwan, remanent magnetization, transpression, Hsuehshan range

INTRODUCTION

Most sedimentary and metamorphic rocks are inhomogeneous and show variations in

composition and physical properties. In many examples, this inhomogeneity is usually in the form of a dominant planar anisotropy, (bedding and fissility in sediments, foliation in slates and schists) or planar discontinuities (such as fault zones, dykes and veins). Depending on the physical conditions that prevail at the time of deformation, brittle and ductile deformation can occur together (Rutter, 1986). This is the case in the particular context of oblique convergence and rotation tectonics considered in this paper.

Rock deformation may lead to the development of orientation anisotropy (Ramsay and Huber, 1983). This fabric anisotropy is sometimes well recorded in other types of physical anisotropy. One of these is the anisotropy of remanent magnetization (RM) that can also provide valuable information on kinematics (Lee *et al.*, 1998).

Several major modes of anisotropic deformation may occur simultaneously, as proportions, in the progressive deformation. However it is poorly understood. This was well demonstrated in northeastern Taiwan, where a very thick series of Paleogene clastic sediments underwent complex deformation during the late Cenozoic Taiwan collision. Here, we describe some characteristics of the anisotropic deformation and show how these various deformation mechanism are recorded in terms of structural history.

GEOLOGIC SETTING

The island of Taiwan is located along the plate boundary between the Eurasian and Philippine Sea plates, and is situated at the junction of the Luzon Arc on the Philippine plate and the Ryukyu Arc on the Eurasian plate (Fig. 1A). The Philippine Sea plate is being subducted beneath the Eurasian plate along the Ryukyu Trench, and overrides the crust of the South China Sea along the Manila Trench. The Chinese continental margin is oriented about N60°E whereas the Luzon arc trends approximately N10°W, with the Philippine Sea plate moving towards the Eurasian plate in a N55°W direction (Seno, 1977; Seno *et al.*, 1993). This tectonic configuration (Fig. 1A) has resulted in oblique subduction and collision, as discussed by Suppe (1981).

The Taiwan mountain belt has suffered a significant clockwise rotation from central to northern Taiwan. Tan (1977) first described the bending of the Taiwan arc; Suppe (1984) interpreted it as the result of flipping of subduction direction and the opening of the Okinawa Trough.

Lue *et al.* (1991) and Lee *et al.* (1991) show that the northern Taiwan has undergone an average clockwise rotation of approximately 20°, over a considerable area. Their results support the idea that the 40°-60° change in the present-day trends across the northern Taiwan includes both a 20°-30° rotation of blocks and an initial induced curvature of 20°-30° (Angelier *et al.*, 1990; Lu *et al.*, 1995) (Figs. 1 B and C).

Geological structures in the Late Cenozoic succession of northern Taiwan are characterized by NE-trending folds and thrust faults, which are generally deformed by strike-slip faults (Fig. 2A). Normal fault systems, which in the most cases postdate the compressional structures, are also present (Lu *et al.*, 1995). Some folds and thrusts are arranged oblique to the regional trend of the belt (20-30° counterclockwise), especially near 121°40'E between Taipei and Ilan. This shows an en echelon pattern that is consistent with a dextral component of strike-slip motion.

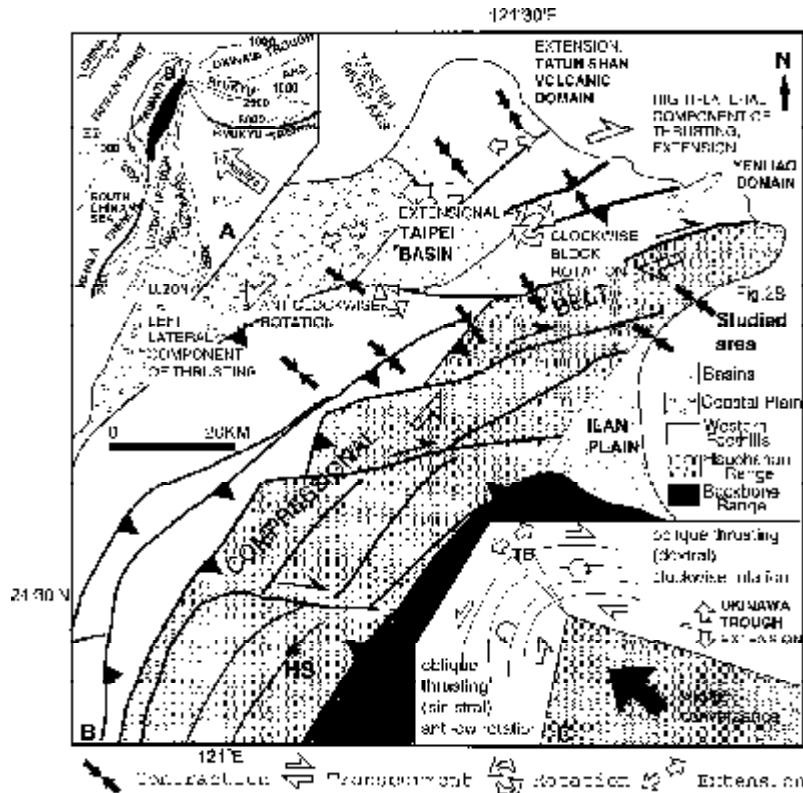


Figure 1. (A). General tectonic map of Taiwan (upper left corner): Isobaths in meters, large open arrow showing the direction of convergence (Philippine Sea plate (PSP) relative to Eurasia (EP). (B). Main tectonic units and Plio-Quaternary tectonic deformation in the foreland thrust belt of northern Taiwan. (Compiled from Ho, 1986; Biq, 1989; Lu *et al.*, 1995). Note the existence of three major domains: (1) the eastern domain characterized by oblique-slip thrusts superimposed by major dextral strike-slip and bulk clockwise rotation deformation; (2) the central domain characterized by indentation and extensional deformation; (3) the western domain where major sinistral oblique thrusting superimposed by dextral bookshelf type strike-slip and bulk anticlockwise rotation dominates. Major thrust faults as heavy lines with triangles on the upthrust side. HS: Hsuehshan.

The Hsuehshan Range (Fig. 1B) consists of a Eocene to Miocene passive margin marine sequence (Ho, 1975; Ho, 1986; Huang, 1980; Tang and Yang, 1976; Teng *et al.*, 1988) characterized by rift and transgressive facies succession (Sun, 1982; Wang, 1987; Lu *et al.*, 1991). Structural analyses (e.g., Tsan, 1976; Lu *et al.*, 1994; 1995; 1997;) have shown that the northern portion of the Hsuehshan Range experienced a complex deformation history that records the stages of contraction, transcurrent faulting, block rotation, and extension. In addition, the entire Hsuehshan Range was uplifted as a pop-up structure in the Taiwan Orogeny (Clark *et al.*, 1993; Chu *et al.*, 1996; Lee *et al.*, 1997; Lu *et al.*, 1997). It suffered intense shortening toward the northwest as well as substantial vertical thickening (Lu *et al.*, 1997).

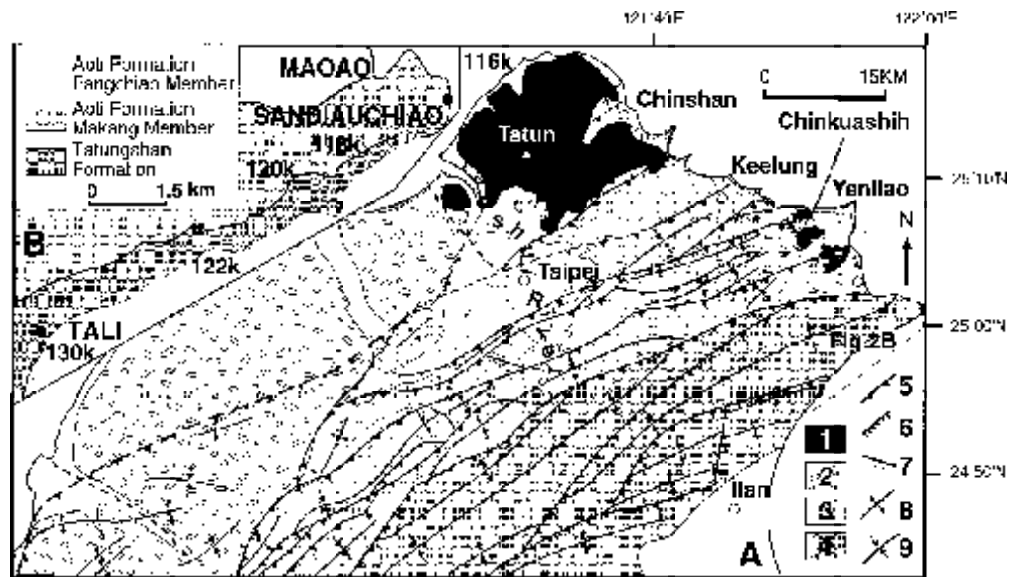


Figure 2. (A). Geological and location map of study area, the numbers show the location of kilometer marks on highway. (B). General structures and megascopic division of northern Taiwan (Lu, *et al.*, 1995). Keys: 1. Pleistocene volcanic rocks; 2. Pleistocene conglomerate; 3. Western Foothills; 4. Hsuehshan Range; 5. thrust fault, 6. normal fault, 7. strike-slip fault, 8. anticline axis, 9. syncline axis,

Lu *et al.* (1994) described a variety of meso-scale structures in northern Taiwan, and interpreted them as resulting from transpression. Lee *et al.* (1998) illustrated the effects of local block-rotation, and hence provided new insights into the relative timing of magnetization and the regional metamorphism/deformation. However, little was known about the geological and tectonic significance of these complicated folds and faults.

In this paper, we focus on new structural data collected in a thick Oligocene sequence, that suffered deformation and very low P/T metamorphism during the Late Cenozoic (Fig. 2B). These strata well exposed in outcrops within wave-cut platforms and are observed over a distance of several kilometers.

DEFORMATION STRUCTURES

A variety of deformation structures highlight the complexity of the multiphase deformation in the study area and provides grounds for elucidating the nature and evolution of the tectonism. We first describe the main deformation structures and then try to establish their relative deformation stages.

Pencil structure and spaced cleavage

Pencil structure is a common feature in the argillites of the Hsuehshan Range. It represents an intersection lineation related to a spaced pressure solution cleavage and a bedding parallel fissility. Therefore, the axis of pencil structure is likely to be formed roughly perpendicular to the axis of regional shortening direction.

Spaced cleavage is widespread in the metasandstone units of the study area. The cleavage

is spaced 1-2 cm and produces a phacoidal or lenticular fabric in sandstones.

One major characteristic of the pencil structure is the consistent trend throughout the northeastern coast of Taiwan. This geometrical homogeneity suggests that the pencil structure and spaced cleavage were younger than most of the other deformational structures, in the study area.

Folds

Folds are the most regional structures in northeastern Taiwan. They are separated into three groups: (1) regional folds with wavelength from several hundred meters to several kilometers; (2) folds of one meter to several hundred meters wavelength associated with strike-slip faults; (3) drag folds of one meter to several hundred meters size associated with SE-vergent thrust faults. The folds of the first group are visible in the regional structural map (Fig. 2A) and their axes generally trend $N60 \pm 20^\circ$. These large folds control the topography of the curved mountain belt and record the regional shortening associated with the collision. The folds of the second group result from a combination of strike-slip faulting and thrust faulting that gave rise to local drag of the folding of layers adjacent to fault zones; some of these folds are larger in wavelength, and the en-echelon folds with NE trends (Fig. 2) may also have formed during the second generation. In the study area most of these folds have axes that trend $N20 \pm 20^\circ$ E. Most of the folds are asymmetric and verge NE. The attitude of the folded bedding may be rotated up to 120° according to the paleomagnetic analysis (Fig. 3). The third group comprises ESE-vergent folds. Some of these ESE-vergent folds in association with ESE-vergent thrusts clearly deformed small west-vergent thrusts (Fig. 4B).

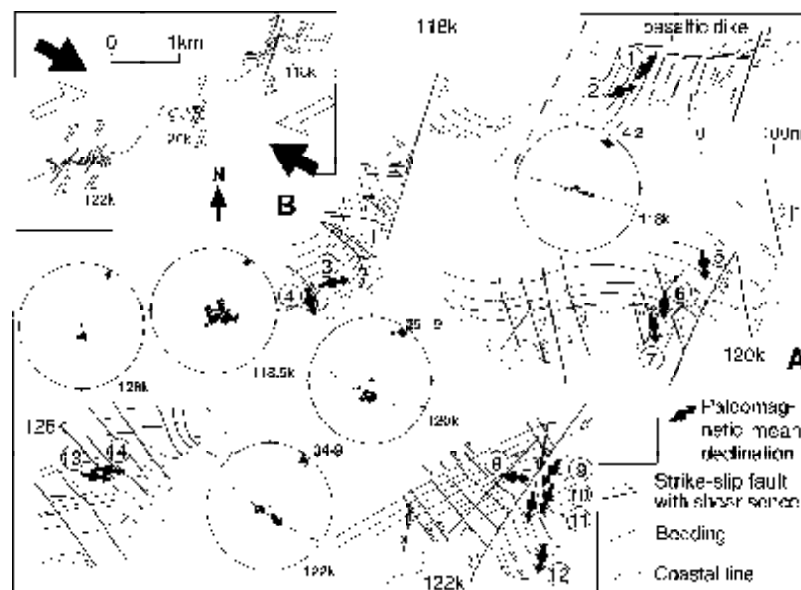


Figure 3. (A). Structural sketches of outcrops, locations of paleomagnetic samples sites (indicated by circled number) and lower hemisphere projection of bedding and pencil structures in the study area: round dot: pole of bedding plane; star: pencil structure lineation; dashed great circle: best-fit great circle of cylindrical fold; square: calculated fold axis; the number at upper-right of diagram represents the bearing and plunge of fold axis. (B). Synoptic map shows a regional dextral transpressional deformation resulting in an oblique stretching anisotropy. Thick solid arrows: contraction, coupled open arrows: transcurrent deformation.

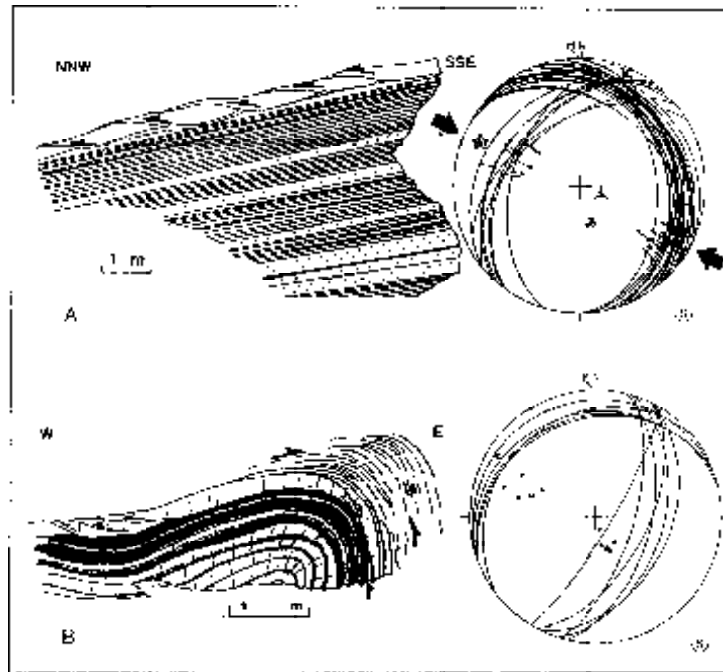


Figure 4. Anisotropic deformation of study area; (A). Sketch and fault-slip analysis of a duplex structure at 138.4K, imbricated thrusts are well-developed in the relatively thick (20~50 cm) layers of sandstone units while pencil structures prevail in the argillite unit. (B). Sketch and projection of bedding plane of east vergent fold, which superposed on the structures described in Figure 5A. Note the curved west vergent thrust at the fold hinge zone. Fault-slip analysis is shown by Schmidt's lower hemisphere projections of fault planes (solid girdles). In Figure 4A, slickenside lineations are shown as small dots with thin centrifugal arrows (normal slip) and centripetal arrows (reverse slip). Small circles represent the pole of the local bedding. Large black arrows indicate directions of compression. Principal axes of paleostress reconstructed based on fault-slip analysis: Five-, four-, and three-pointed star (maximum compressional stress σ_1 , intermediate stress σ_2 , and minimum stress σ_3 respectively). Open circles indicate the poles of the bedding plane. Numbers at the upper right corner of projection diagram show the bearing and plunge of fold axis.

Thrust Faults

Thrust faults are common in the study area. Conjugate sets of thrusts, imbricated thrusts, and bedding-parallel thrusts have been recognized. The thrust faults form flat-ramp-flat geometries with ramps within competent beds (Fig. 4A). It has been noticed that when the WNW-vergent thrust faults and the ESE-vergent thrust faults occur as a conjugate systems, the ESE-vergent faults often cut through and offset the WNW vergent faults.

Oblique reactivation of the thrust is revealed by the presence of multiple sets of striations on fault surface. Crosscutting relationships often suggest that the older striations are dip-slip, whereas the younger striations record oblique slip (Angelier *et al.*, 1990; Lu *et al.*, 1995).

Strike-slip faults

Minor and meso-scale faults with apparent strike-slip displacements can easily be detected in plan view on coastal wave-cut platforms and recognized by offsets of the bedding along planar surfaces that display strike-slip striations. The amount of horizontal displacements of the strike-slip faults generally ranges from centimeters to decimeters (Fig. 5). Typically, the sense of motion may be indicated by offset layers, drag folds and, in some cases, en-echelon tension gashes or veins. There are also examples that recorded dextral and sinistral slip on a single fault surface. Our results based on field observation on the strike-slip faults was supported by the analysis of aerial photographs (scale 1:5,000) and led to the following conclusions:

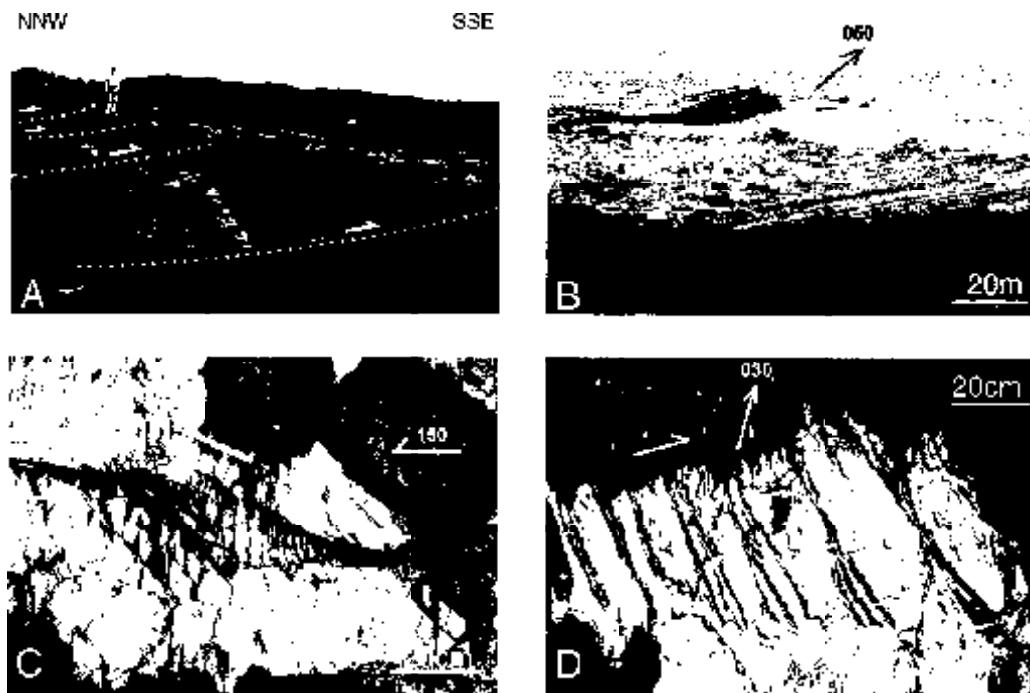


Figure 5. Bookshelf type strike-slip faults and transpressive structures in northeastern Taiwan; (A). Sinistral bookshelf type strike-slip faults at 122K. Dot lines indicate the fault traces, arrows mark the slip sense (see Figure 3B for location); (B). Dextral pressure ridge at 117.5K, dot line indicate the hinge part of pressure ridge; (C). Left lateral rhomb horse with compressive horse tails at 121K; D. Dextral strike-slip movements (indicated by small lateral drag folds) in association with left lateral retaining oversteps at 122K, black line marks trace of pencil structure. Numbers indicate the direction of structures.

First, strike-slip faulting occurred at regional scale as conjugate sets of strike-slip faults (major ENE-WSW dextral and minor NNW-SSE sinistral). This group of strike-slip faults apparently developed during regional-scale folding, with one of the inferred stress axes (σ_3) being sub-parallel or slightly oblique to the regional fold axes. Their fault planes often merge with a regional scaled thrust (Figs. 1 and 2). This geometry resulted in a domino style of deformation often associated with dextral shear.

The second group of strike-slip faults is in association with the meso-scale drag folds (Fig. 3B, e.g. the outcrops 128K, 122K and 120K) occurring as fractures along the hinge area of the drag folds. Orientation of these faults ranges between N10°E and N50°E and most of the faults display dextral offsets. In contrast, most of the faults on the fold limbs associated with the bookshelf style of deformation, have sinistral slip (Fig. 5A) and range in orientation from N130° to N160°. Transpressive structures are also associated with this second group of faults and include pressure ridges (Fig. 5B), push-ups and rhomb horses (Fig. 5C) associated with restraining bands and restraining oversteps (Fig. 5D) (terms after Biddle and Christie-Blick, 1985). This range of structures suggests that regional deformation is diffusely accommodated by ductile, brittle-ductile to brittle strike-slip shear zones, lateral thrusts, and backthrusts (Figs. 1B and 3B).

The third group of strike-slip faults are more brittle in character and occurs associated with veins and joints. Veins related to strike-slip movements commonly form en-echelon patterns along or near strike-slip faults. Along several shear zones, sets of en-échelon veins generally indicate a sense of motion consistent with other observations. For example, at the outcrop 130K (Figure 6, see also location in Figure 2B), two sets of dextral en-échelon quartz veins strike about 080°E and 060°E (a and b in Figure 6 A(C)) and three sets of bedding thrust striations trend 150°E, 130°E and 105°E on average (1,2, and 3 respectively in Figure 6A(C)). The veins that trend 080°E were cut and displaced by the minor thrusts, whereas the quartz veins that striking 060°E cut through the thrust surfaces. These relationships indicate that most thrusts formed first (Fig. 6A(A)), with slip vectors trending about 105-110°E (in the present-day configuration). Later, the thrust planes underwent oblique thrust reactivation and the dextral veins striking 060°E developed (Fig. 6A(B)). Note that this succession may reveal regional changes through time in the direction of compression, but can also be interpreted in terms of rotation within a constant stress field. A likely possibility is that block rotation occurred after the development of the first set; while block rotation continued (about 20° of clockwise rotation), new thrusting took place episodically, resulting in successive reactivations. The latest stage in the deformation process is represented by the youngest set of dextral en echelon veins, which crosscut the previous brittle structures. Note also that at the same outcrop some sets of sinistral en-echelon fractures are curved, and only one pressure solution cleavage is observed. The above sequence of deformation may indicate that there is a progressive clockwise rotation tectonics. During the rotational process, the orientation of the maximum horizontal stress remained the same while the 105°E striations was rotated to 130°E and finally 150°E, the 060°E quartz veins being rotated to 080°E direction.

INSIGHTS FROM ANISOTROPY OF REMANENT MAGNETIZATION (RM)

Paleomagnetic results (Lee *et al.*, 1998) indicate that the directions of the natural remanent magnetization (NRM) are close to the strike of the folded strata (Tab. 1). This correlation suggests that NRM may result, at least in part, from the compression associated with the regional deformation. Fourteen sites were chosen, where slightly metamorphosed sedimentary strata that underwent multiple deformation events characterized by drag folds and densely spaced faults, for the present paleomagnetic study (Fig. 3). We perform NRM measurement to check whether there was rotation of NRM during the rotational deformation.

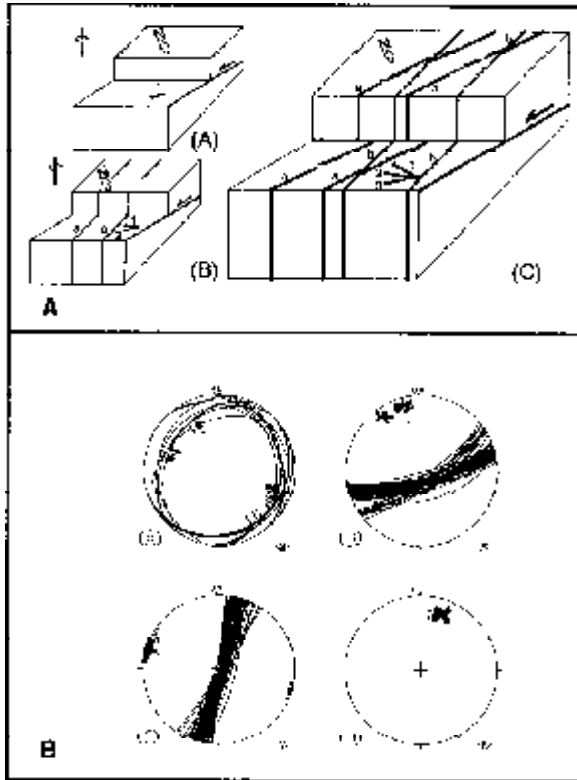


Figure 6. (A) Crosscutting relationships between thrust, and quartz veins in association with dextral movement during block rotation. (A) Development of bedding thrust with striation. (B) First set of quartz veins (a) in association with dextral movement, indicated by an echelon segments. (C) Present state development of the second set of quartz veins (b) and progressive deformation.

At least eight samples per site were examined using 2G Enterprise cryogenic magnetometer (model 755 SRM) in a magnetically shielded room. The specimens were stepwisely thermally demagnetized from room temperature up to about 510°C. Thermal demagnetization was conducted with a Schonstedt TSD-1 thermal demagnetizer. The ambient magnetic field in the cooling chamber of TSD-1 was below 2-nT. Low field magnetic susceptibility of the specimens was measured repeatedly after each heating step to monitor whether there was compositional change of the magnetic minerals during demagnetization.

The results of NRM studies show that the paleo-inclinations are negative at all sites (I_g and I_s in Table 1), suggesting that the characteristic paleomagnetic polarity were acquired during magnetic time zone of reversed polarity. The paleo-declinations measured, however, are very scattered (D_g and D_s in Table 1). To better analyze these NRM orientations, we also examined the results in the pre-folding reference coordinates. For this purpose, a bedding correction was made by tilting the bedding plane back to horizontal. Unfortunately, no reliable fold test could be made in the study area because all of the large folds are disrupted or do not exhibit two steeply dipping flanks. However, it is important to note that, because most large folds are cylindrical with horizontal axes (Fig. 3), it is reasonable to assume that simple backtilting correction effectively restores the pre-folding position. After making the tilt corrections (D_s and I_s in Table 1), the paleo-declinations still show random distribution. Nevertheless the strike

-corrected paleo-declinations were within acceptable accuracy and reasonable consistency in a direction oblique of about $30 \pm 10^\circ$ clockwise (Φ_s in Table 1) to the bedding strike in the studied sites. Although this direction (negative inclination with north seeking declination) is quite unusual at northern hemisphere, there are several possibilities for it. Lee *et al.* (1998) proposed that NRMs might be remagnetized in a very early stage and formed remanent anisotropy under tectonic compression. This supposes that NRM was acquired during the same time period, and predated much of the deformation. Results from sites 3, 4, 9 (Tab. 1) show higher values of Φ_s , Φ_g , θ than at the other sites, due probably to relatively densely distributed strike-slip movement in these sites (Fig. 3).

The Dec* values correspond to declinations deduced by rotating the bedding strikes at each site (column 3, Table 1) in order to be parallel to the regional trend of the mountain belt (N10°E), assuming that vertical axis corrected declination pointed (Oligocene) north. Applying rotations that put the strikes of stratigraphic bedding along N10°E direction, one observes that most corrected paleomagnetic directions point in average direction of N48°E (see Table 1).

Table 1. Paleomagnetic results of the shear zone of Hsuehshan Range at north-eastern coast of Taiwan.

Site number	N	Bedding	Ds	Is	Φ_s	ks	α_{95s}	Dg	Ig	kg	α_{95g}	Dec*	θ
2	5	030/08°N	46.4	-55.2	16.4	31.4	8.8	40.7	-36.5	51.5	8.8	26.7	20
	8	022/15°N	60.8	-37.4	33.8	13.0	11.9	50.7	-42.8	19.9	11.9	48.8	12
3	5	030/15°N	86.4	-32.8	56.4	25.0	33.9	75.0	-31.4	35.0	33.9	56.4	30
4	7	075/15°N	156.7	-27.7	81.7	25.0	11.4	154.5	-45.0	24.9	11.4	91.7	65
5	10	140/42°E	176.8	-18.2	36.8	34.3	9.5	155.5	-7.9	34.4	9.5	45.8	130
6	10	145/45°E	189.2	-22.5	34.2	18.8	10.8	160.5	-46.5	18.7	10.8	44.2	145
7	8	130/16°E	171.5	-41.3	41.5	43.5	7.9	157.6	-53.4	43.5	7.9	51.2	120
8	0	075/20°N	98.4	-30.5	28.4	24.7	9.6	73.7	-44.9	33.7	9.6	38.4	60
9	7	170/20°E	229.8	-18.8	50.8	57.4	7.4	224.2	-25.6	57.6	7.4	69.8	160
10	11	165/10°E	207.8	-20.8	42.8	46.1	6.5	215.3	-31.9	46.4	6.5	52.8	155
11	13	170/10°E	194.3	-26.6	34.3	26.3	7.9	186.4	-31.8	26.3	7.9	34.3	160
13	6	160/10°E	193.4	-27.3	33.4	17.6	11.9	189.2	-34.6	17.6	11.9	33.4	150
12	7	080/15°N	99.5	-30.4	19.5	46.9	8.2	90.2	-34.2	46.9	8.2	29.5	70
14	10	070/10°N	93.0	-34.2	22.0	22.2	9.9	89.8	-45.5	22.2	9.9	33.0	60
			Mean		32.5							48.3	
			stdev.		13.2							17.8	

N : number of sample for Fisher statistics
 Ds&Is : site mean declination and inclination after tilting correction
 Dg&Ig : site mean declination and inclination before tilting correction
 ks&kg : precision parameter for Fisher statistics after and before tilting correction respectively
 α_{95s} & α_{95g} : 95% confidence interval for Fisher statistics after and before tilting correction respectively
 Φ_s : Ds-(strike of bedding)
 Φ_g : Dg-(strike of bedding)
 Dec* : new Dec. (Ds-10 : when the strike of bedding rotated to N10°E)
 θ : rotation angle of the structures relative to the bedding N10°E (- : clockwise ; + : counterclockwise)
 Diagrams: lower hemisphere equal-area projections of site mean declination and inclination before tilting correction(A), after tilting correction(B) and after strike correction(C).
 #: site 4 not include in the means, stdevs. & projections for eliminating statistic bias



Previous tectonic studies (e.g. Angelier *et al.*, 1990; Lu *et al.*, 1995) demonstrated the main characteristics of the major compression related to the Late Cenozoic Taiwan collision. These results reveal that a compression direction trend is about N130°E. Our corrected NRM axes, however, are approximately sub-perpendicular to this trend. This fact is important because it suggests that the development of NRM predated the late stage deformation and disruption of the folds.

The corrected paleomagnetic orientations do not record normal and reversed polarity epochs of depositional age, Oligocene, of succession. This observation suggests that little remains of the primary component of NRM acquired during the deposition of the formations. It is therefore proposed that magnetization occurred during a regional low-grade metamorphic event that probably affected the entire study area during the early stages of deformation.

INSIGHTS FROM EXPERIMENTAL MODELS

Recent 3-D sandbox models (Lu and Malavieille, 1994; Lu *et al.*, 1998) indicated that oblique indentation and rotation models account well for the kinematics and tectonic pattern in the Taiwan thrust wedge (see Figure 1B).

The effect of collision with a corner indenter lies in the development of an asymmetrical thrust wedge structure in different tectonic domains (Fig. 1C). In northern Taiwan the deformation is relatively complex and involves both extension and normal faulting as pointed out by Lu *et al.* (1995). In the study area, however, partitioning only involves thrusting and strike-slip faulting. Experimental modeling suggests that faults or shear zones are rotated around the indentation point by transcurrent faulting processes. Figure 8 shows the inferred evolution of the northern segment of the Taiwan belt. As inferred from the results of experimental modeling, the northern segment of the Taiwan belt is believed to have suffered first contractional deformation (with fold-thrust shortening and oblique thrust-sheet stacking, Figure 7A), then oblique thrusting and finally dextral transcurrent faulting at the latest stage (Figs. 7B and C). Figure 8D indicates the successive locations of the indenter at stage A, B, and C. At the third stage, transpressional deformation accommodated the shortening and vertical thickening of thrust faults.

DISCUSSION AND CONCLUSION

A first aspect of the structure that deserves explanation is the complexity of the fracture patterns in the study area. According to the paleomagnetic measurements (Tab. 1), the strata in the study area locally suffer rotations up to 160°. Although the system of rotated blocks cannot be reliably restored, the existence of these rotations provides a simple explanation for the complexity in brittle deformation. During the rotation of blocks, new fracture systems developed when the previous ones could no longer accommodate slip within the new stress field. For instance, Figure 8A shows a compilation diagram illustrating en-echelon structures characteristic of dextral transcurrent zones evolving during simple shear (after Hancock, 1985). After a 30° clockwise block rotation (Fig. 8B) a new set of en-echelon structures develops if

the rotation occurs abruptly and affects the previous structures. Note that a new foliation (f) overprints the old sinistral X-shear fracture, and that new extension cracks (e) overprint old dextral R'-shears (Fig. 8B). If the finite rotation becomes larger than 30° , some strike-slip structures may even move in opposite sense (change from dextral to sinistral or vice versa). This is the general case of brittle and brittle-ductile structures in the study area, (e.g. Figure 6). Most sinistral shear fractures are sub-parallel to the pencil structure related to pressure solution cleavage, whereas the dextral fractures and extension cracks are subparallel.

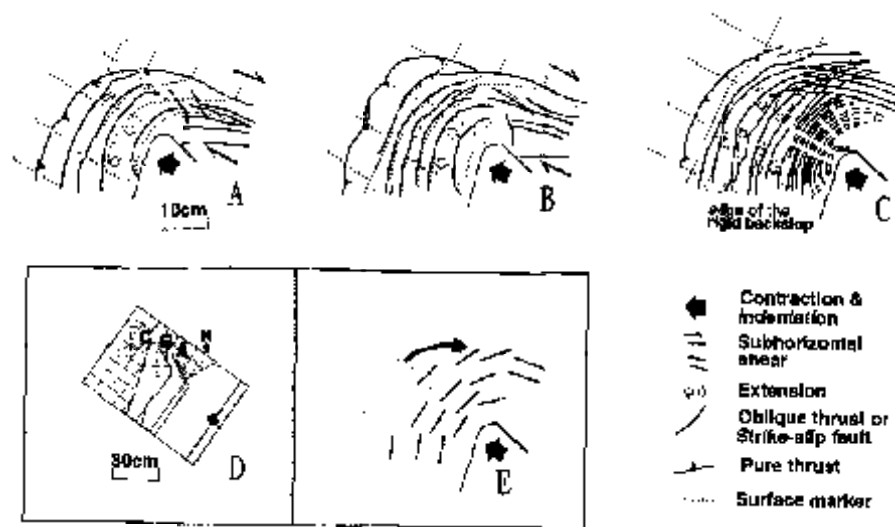


Figure 7. Results of sandbox experiment (A). Contractional deformation with fold-thrust shortening and oblique thrust-sheet stacking, (B). Oblique thrusting and dextral transcurrent faulting. (C). Transpressional stretching accommodated the closing of the thrust spacing and the development of pure strike-slip faults. (D). Sandbox model (modified from Lu and Malavieille, 1994). (E). Interpretative sketch shows the extrusion of the material and the change of structure attitude during the oblique collision and indentation tectonics.

It is surprising to see that the formation of the pencil structures and fracture cleavages appears to postdate those of other structures, because they are generally considered as occurring at an early stage of deformation. However, there is no doubt that left regarding the young age of these structures because of their penetrative and uniform orientation regardless of the complexity and variable orientation of the earlier structures. To reconcile this observation, we propose that during the rotational deformation the orientation of ductile structures (e.g. cleavage) were progressively reoriented continuously so that they remained perpendicular to the maximum horizontal stress. In contrast, the brittle structures (e.g. faults and veins) were not reoriented and thus record multiple deformation events.

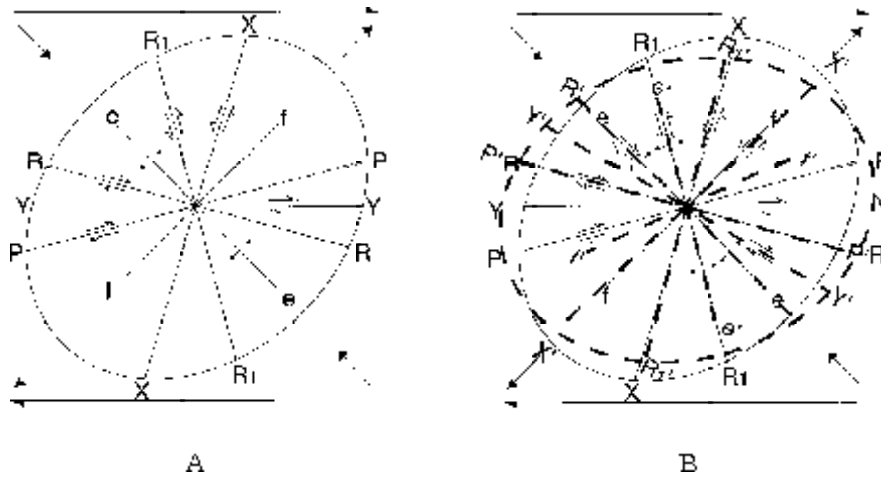


Figure 8. (A). Compilation diagram illustrating en echelon structures characteristic in dextral transcurrent zones under simple shear (after, Hancock, 1985). R and R1, Riedel and conjugated Riedel shears, P, X and Y, P-, X- and Y- shears; e, extension joint, fissure or vein; f, fold axis, cleavage or other foliation. (B). After a 30° clockwise block rotation a new set of en echelon structures superposed on the previous structures. Note that new foliation (f) is overprint on the old sinistral-shear fracture, new extension crack (e) is overprint on the old dextral R'-shear.

As summarized in Table 2, the deformation process in the study area shows a sequence which is much distinct from what expected for a general deformation of rigid succession. Instead we point out that most structures developed in the frame of progressive indentation in northeastern Taiwan (Fig. 7). Note that in Table 2 the remagnetization may correspond to the initial stage of pressure solution.

Table 2. Structure evolution of northeastern coast of Taiwan.

	Oligo-Miocene -- Pleistocene Recce
1. Thrust faults & folds	?-----??
2. Remanent magnetic anisotropy	?----?
3. Transcurrent, block rotation	?-----
4. Back folding & back thrusting	???-----?
5. pressure solution cleavage (pencil structure and spaced cleavage)	?-----?

The 50° clockwise rotation observed around the indented backstop in a sandbox model (Lu and Malavieille, 1994) suggests that extrusion or escape tectonism may have occurred in association with ductile shear on the right side of the indenter (Fig. 7E). This ductile shear regime may have rotated and transferred the rock fabrics from trending approximately NE-SW to E-W trends in the case of northern Taiwan. According to Angelier *et al* (1990) and Lu *et al* (1995) the curvature in the Hsuehshan Range can be the result of partially (about 30°) an initial change of the structural trend without block rotation and partially block rotation. However, NRM data then pointed to present north, show a N10°E trend. This implies that the original trend of strata in the studied area may have been NE-SW. This conclusion agrees well with that suggested by the paleomagnetic data. This can elucidate why we need a back rotation to replace NRM axes sub-perpendicular to the compressional direction.

Transpression is a consequence of oblique plate convergence (Dewey *et al.*, 1998). Within a convergent plate boundary zone, compressional strains are generally accumulated in the displacement zones that bound units of less-deformed material on several scales. In this paper, transpression is defined as strike-slip deformation that deviates from simple shear because of a component of shortening nearly orthogonal to the deformation zone. Figure 9 schematically illustrates the three main stages of transpression, which include (1) early contraction and volume loss; (2) oblique transcurrent deformation with significant rotation producing oblique stretching deformation and dominant dextral shear zones; and (3) a late stage of compression in association with pop-up structure development and backthrusting. As summarized below, it is suggested that such a scenario of multistage deformation accounts well for the structural development and tectonic evolution in northeastern Taiwan.

Based on structural and tectonic analyses, paleomagnetic studies, and physical models, we propose three stages of deformation for northern Taiwan.

(1) During the first stage, contraction prevailed in response to collision and indentation (Figs. 8A and 10A). The predominant structural development involved thrusting, regional tilting of strata, and folding. This early deformation probably occurred prior to complete lithification and as a result NRM fabrics generally overprint these structures.

(2) During the second period, general shear (Hanmer and Passchier, 1991) became predominant because frontal contraction could not be easily accommodated (Figs. 8B and 9B). Thus, in the eastern wing of the Hsuehshan belt dextral shear predominated, because lateral escape was possible and resulted in development of strike-slip shear-zones and drag folds accompanying progressive oblique thrusting. A variety of domino-type and bookshelf-type strike-slip structures developed at this stage, as well as numerous transpressional structures such as pressure ridges, restraining oversteps and rhomb horses. It is therefore inferred that most of the clockwise rotation, as revealed by paleomagnetic studies, took place in this stage.

(3) The last period principally involved transpressional deformation with vertical extension (Figs. 8C and 9C). It resulted in backthrusts, in association with pop-up structures at various scales (including that of the whole Hsuehshan Range). The penetrative pencil structures and spaced cleavages also developed at this stage.

In summary, the deformation of the Tertiary succession at the northern tip of the Hsuehshan Range, involves three stages of deformations that all belong to the same major collision related event. Based on comparison between the results of the paleomagnetic and tectonic analyses,

the formation of remanent magnetization occurred before the second folding stage and at the same time or soon after the first folding stage. An interesting aspect of the deformation is that ductile structures deformed and migrated continuously in the rotation tectonics and hence remained perpendicular to the maximum horizontal stress, resulting in a single nearly homogeneous structural pattern. In contrast, the brittle structures developed episodically into several stages as a function of increasing deformation, resulting in a more complex structural pattern.

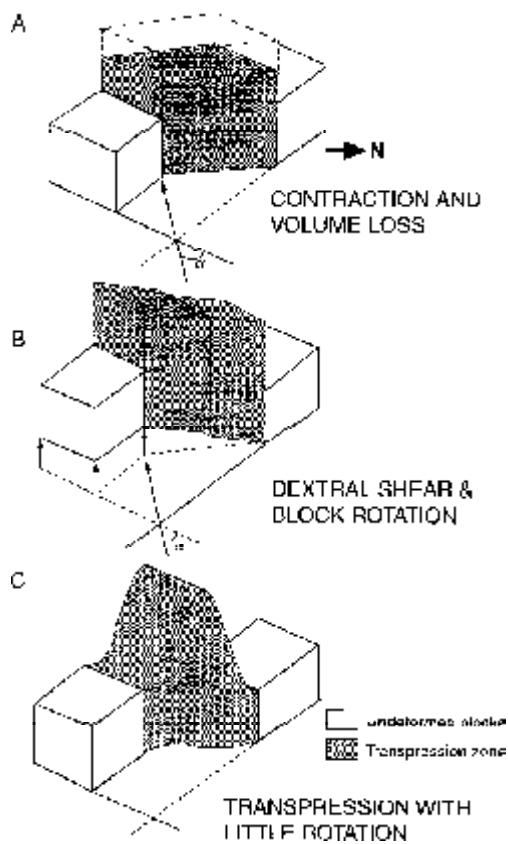


Figure 9. Three stages of strain models correspond to the transpressional tectonics. (Modified from Dewey, *et al.* 1998). (A): contraction; (B): dextral shear and block rotation; (C): transpression with vertical extension. Similar characteristics of kinematics of anisotropic deformation are clearly shown in the study area (see text). α : oblique convergent angle.

ACKNOWLEDGMENTS

This research was benefited from a NSC support (grant NSC88-2116-M002-018). We thank Jacques Malavieille, Don Fisher, Tim Byrne, Yuchang Chan, En-Chao Yeh, Tetsuzo Seno and Soh Won for their valuable comments, which have improved the manuscript. and two reviewers Lo, Ching-Hua and Horng Chong-Shem, for revising this manuscript.

REFERENCES

- Angelier, J., Bergerat, F., Chu, H.T., and Lee, T.Q. (1990) Tectonic analysis and the evolution of a curved collision belt: the Hsuehshan Range, northern Taiwan: *Tectonophysics*, **183**(1-4), 77-96.
- Biddle, K.T., and Christie-Blick, N. (1985) Glossary-strike-slip deformation and basin formation and sedimentation. In K.T. Biddle, and N. Christie-Blick, Eds. Strike-slip deformation, basin formation, and sedimentation: *Exxon Prod. Res.*, **37**, 375-386.
- Biq, Chingchang, (1989) The Yushan-Hsuehshan megashear zone in Taiwan: *Proc. Geol. Soc. China*, **32**(1), 7-20.
- Chu, H.T., Lu, C.Y., Lee, J.C., and Lin, N.T. (1996) Contractional, transcurrent, backthrusting and extensional tectonics: Examples from Hsuehshan Range (in Chinese, with English abstract): *Ti-Chih*, **15**(2), 61-68.
- Clark, M.B., Fisher, D.M., Lu, C.Y., and Chen, C.H. (1993) Kinematic analyses of the Hsuehshan Range, Taiwan: A large scale pop-up structure: *Tectonics*, **12**, 205-217.
- Dewey, J.F., Holdsworth, R.E., and Strachan, R.A. (1998) Transpression and transtension zones. In R.E. Holdsworth, Strachan, R. A., Dewey, J. F., Ed. Continental Transpressional and Transtensional Tectonics: *The Geological Society*, London, **135**, 1-14
- Hancock, L. (1985) Brittle microtectonics; principles and practice: *Journal of Structural Geology*, **7**, 3-4, Geological Survey of Canada 437-457,
- Hanmer, S. and Passchier, C. (1991) *Shear-sense indicators: a review*, Cat. No. M44-90/17E., 90-17, Ottawa, 72 p
- Ho, C.S. (1975) An introduction to the geology of Taiwan: explanatory text of the geologic map of Taiwan: *Ministry of Economic Affairs*, R.O.C., 153.
- Ho, C.S. (1986) A synthesis of the geologic evolution of Taiwan: *Tectonophysics*, **125**, 1-16.
- Huang, T.C. (1980) Oligocene to Pleistocene calcareous nannofossil biostratigraphy of the Hsuehshan Range and western foothills in Taiwan: *Geol. Paleont. SE Asia*, **21**, 191-210.
- Lee, J.C., Angelier, J., and Chu, H.T. (1997) Polyphase history and kinematics of a complex major fault zone in the northern Taiwan mountain belt: the Lishan Fault: *Tectonophysics*, **274**, 97-115.
- Lee, T.Q., Angelier, J., Chu, H.T., and Bergerat, F. (1991) Rotations in the northeastern collision belt of Taiwan: Preliminary results from paleomagnetism: *Tectonophysics*, **199**, 109-120.
- Lee, T.Q., Lee, J.C., Chu, H.T., Lu, C.Y. and Hu, J.C. (1998) Paleomagnetic study in a folded zone of Hsuehshan Range, northeastern coast of Taiwan: *TAO*, **9**, 643-655.
- Lu, C.Y., and Malavieille, J. (1994) Oblique convergence, indentation and rotation tectonics in the Taiwan Mountain Belt: Insights from experimental modeling: *Earth and Planetary Sciences Letters*, **121**, 477-494.
- Lu, C.Y., Lee, J.C., and Lee, J.F. (1991) Extensional and compressional tectonics in central Taiwan. In J. Cosgrove, and M. Jones, Eds. Neotectonics and resources, Chapter 6, 85-92. Belhaven Press, London and New York.
- Lu, C.Y., Chen, Y., and Chu, H.T. (1994) Transpression structures in northern Taiwan: a case study of the coast between Maoao and Tali: *Ti-Chi*, **14**, 45-62, (in Chinese with English abstract).

- Lu, C.Y., Angelier, J., Chu, H.T., and Lee, J.C. (1995) Contractional, transcurrent, rotational and extensional tectonics: Examples from northern Taiwan: *Tectonophysics*, **246(1-3)**, 129-146.
- Lu, C.Y., Chu, H.T., and Lee, J.C. (1997) Structural evolution in the Hsuehshan Range, Taiwan: *Jour. Geol. Soc.*, **40**, 261-279.
- Lue, Y. T., Lee, T.Q., Hong, C.S., and Wong, Y. (1991) Magnetic fabric in the non-metamorphosed terrain of the northwestern foothill-Hsuehshan belts of Taiwan: *Proc. Geol. Soc. China*, **34**, 131-146.
- Ramsay, J.G. and Huber, M.I. (1983) *Strain analysis. The Techniques of Modern structural Geology*, **1**, Academic Press, 700 p
- Rutter, E.H. (1986) On the nomenclature of mode of failure transitions in rocks: *Tectonophysics*, **122(3-4)**, 381-387.
- Seno, T., Stein, S. and Gripp, A.E. (1993) A model for the motion of the Philippine Sea Plate consistent with NUVEL-1 and geological data: *JGR*, **98(10)**, 17941-17948.
- Seno, T. (1977) The instantaneous rotation vector of the Philippine Sea plate relative to the Eurasian plate: *Tectonophysics*, **42**, 209-226.
- Sun, S.C. (1982) The Tertiary basins of offshore Taiwan. 2nd ASEAN Council on Petroleum (ASCOPE) Conference, Manila, 1981, Proc., 125-135.
- Suppe, J. (1981) Mechanics of mountain building in Taiwan: *Memo. Geol. Soc. China*, **4**, 67-89.
- Suppe, J. (1984) Kinematics of arc-continent collision, flipping of subduction, and back-arc spreading near Taiwan: *Memo. Geol. Soc. China*, **6**, 21-33.
- Tan, L. (1977) Pleistocene eastward bending of the Taiwan arc: *Memo. Geol. Soc. China*, **2**, 77-84.
- Tang, C.H., and Yang, C.Y. (1976) Mid-Tertiary stratigraphic break in the northeast Hsuehshan Range of Taiwan: *Petrol Geol Taiwan*, **13**, 139-148.
- Teng, L., S., Huang, C.Y., and Lee, C.T. (1988) On the stratigraphy of the Wulai Group in the Wulai-Pinglin area, northern Hsuehshan Terrain, Taiwan: *Proc. Geol. Soc. China*, **31**, 93-100.
- Tsan, S.F. (1976) The folding and block movement of the Hsuehshan Range, Taiwan: *Bull. Geol. Sur. Taiwan*, **25**, 29-34.
- Wang, Y. (1987) Continental margin rifting and Cenozoic tectonics around Taiwan: *Memo. Geol. Soc. China*, **9**, 227-240.

